Author/s:
Laurens, E;Yeoh, SD;Rigopoulos, A;O'Keefe, GJ;Tochon-Danguy, HJ;Chong, LW;White, JM;Scott, AM;Ackermann, U

Title:
Fluorine-18 radiolabeling of a nitrophenyl sulfoxide and its evaluation in an SK-RC-52 model of tumor hypoxia

Date:
2016-08-01

Citation:
Laurens, E., Yeoh, S. D., Rigopoulos, A., O'Keefe, G. J., Tochon-Danguy, H. J., Chong, L. W., White, J. M., Scott, A. M. & Ackermann, U. (2016). Fluorine-18 radiolabeling of a nitrophenyl sulfoxide and its evaluation in an SK-RC-52 model of tumor hypoxia. Journal of Labelled Compounds and Radiopharmaceuticals, 59 (10), pp.416-423. https://doi.org/10.1002/jlcr.3426.

Fluorine-18 radiolabelling of a nitrophenyl sulfoxide and its evaluation in an SK-RC-52 model of tumor hypoxia

Abbreviated title: F-18 labelled sulfoxide for hypoxia imaging

Evelyn Laurens[1], Shinn Dee Yeoh[2], Angela Rigopoulos[3], Graeme J. O'Keefe[2], Henri J. Tochon-Danguy[2,4], Lee Wen Chong[1], Jonathan M. White[1], Andrew M. Scott[2,3,4,5], Uwe Ackermann[*2,3,4,5]

[1] School of Chemistry and Bio21 Institute, The University of Melbourne

[2] Department of Molecular Imaging and Therapy, Austin Health, Level 1 HSB, 145 Studley Road, Heidelberg 3084

[3] Olivia Newton-John Cancer Research Institute, Melbourne

[4] School of Medicine, Dentistry and Health Sciences, The University of Melbourne

[5] School of Cancer Medicine, LaTrobe University, Melbourne

[*] Corresponding author

Key words:

Hypoxia

Radiolabelling

SK-RC-52 tumor model

Small animal imaging

Abstract

The significance of imaging hypoxia with the PET ligand [^{18}F]FMISO has been demonstrated in a variety of cancers. However, the slow kinetics of [^{18}F]FMISO require a 2 h delay between tracer administration and patient scanning. Labelled chloroethyl sulfoxides have shown faster kinetics and higher contrast than [^{18}F]FMISO in a rat model of ischemic stroke. However, these nitrogen mustard analogues are unsuitable for routine production and use in humans. Here we report on the synthesis and *in vitro* and *in vivo* evaluation of a novel sulfoxide which contains an ester moiety for hydrolysis and subsequent trapping in hypoxic cells. Non-decay corrected yields of radioactivity were 1.18±0.24% (n=27, 2.5±0.5% decay corrected radiochemical yield) based on K[^{18}F]F. The radiotracer did not show any defluorination and did not undergo metabolism in an *in vitro* assay using S9 liver fractions. Imaging studies using an SK-RC-52 tumor model in BALB/c nude mice have revealed that [^{18}F]**1** is retained in hypoxic tumors and has similar hypoxia selectivity to [^{18}F]FMISO. Due to a three times faster clearance rate than [^{18}F]FMISO from normoxic tissue, [^{18}F]**1** has emerged as a promising new radiotracer for hypoxia imaging.

Introduction

The presence of hypoxia is a negative prognostic factor in many solid tumors such as head and neck carcinoma or malignant glioma [1-4]. Over the last few decades, numerous strategies have been developed to overcome therapy resistance of hypoxic tumors. Among those are the use of hypoxia directed cytotoxic drugs, radiosensitizers, intensity modulated radiotherapy, conformal radiotherapy, accelerated radiotherapy with carbogen and nicotinamide (ARCON). [5-11] Functional imaging of hypoxic subvolumes using Positron Emission Tomography (PET) plays a crucial role in order to accurately employ these therapeutic regimens. [12]

PET imaging of tissue hypoxia in humans has been predominantly performed with [^{18}F]FMISO and [^{18}F]FAZA [13-17]. The retention of both radiotracers in hypoxic cells is based on the bioreduction of a nitroimidazole group and it is commonly accepted that FMISO shows uptake in tumors with a pO_2 value of less than 10 mm Hg [18]. However, slow accumulation in hypoxic tissue and slow clearance from normoxic tissue results in a low target to background ratio and a 2 h delay between tracer administration and the actual scanning of a patient [19]. This shortcoming has sparked the development of new tracers for hypoxia imaging. Whilst most research efforts were focused on developing nitroimidazoles with improved pharmacokinetics, our laboratory has synthesised haloethyl sulfoxides as a new class of hypoxia imaging agents [20-24]. The proposed mechanism of trapping is via the bioreduction of the sulfoxide group followed by the formation of a highly reactive aziridinium ion. This aziridinium ion has the ability to alkylate DNA or intracellular molecules, which leads to irreversible trapping and accumulation of radioactivity in the hypoxic cell (Figure 1). Although the 4-nitrophenyl

sulfoxide tracer in particular showed great promise as a hypoxia imaging agent in a stroke model in rats, the routine use of this compound was deemed unsuitable since its structure is closely related to that of the highly toxic nitrogen mustards.

In our attempt to synthesise more suitable 4-nitrophenyl sulfoxide based radiotracers, we modified the chemical structure of the lead compound by replacing one of the chloroethyl groups with an ethyl acetate group.

In this publication, we report on the synthesis, *in vitro* and *in vivo* evaluation of Ethyl 2-((2-[^{18}F]fluoroethyl)(4-(4-nitrophenylsulfinyl)phenyl)amino) acetate ([^{18}F]**1**) in transplanted SK-RC-52 tumor bearing BALB/c nude mice. A direct comparison with [^{18}F]FMISO enabled us to further evaluate the suitability of [^{18}F]**1** as imaging agent for tumor hypoxia.

Materials and methods

General

No-carrier-added [^{18}F]fluoride was produced by the ^{18}O(p,n)^{18}F nuclear reaction with an 18 MeV proton beam generated by the IBA Cyclone 18/9 cyclotron in an niobium target using [^{18}O]H_2O at Austin Health, Centre for PET. Typical irradiation parameters were 38 μA for 50 min, which resulted in 51.8-57.2 GBq (1.4-1.6 Ci) of [^{18}F]fluoride being transferred into the synthesis module. Isolation of the [^{18}F]fluoride ion from [^{18}O]H_2O was achieved by trapping on a QMA ion exchange column. Elution of the column with a solution containing 3.45 mg of anhydrous K_2CO_3 (0.025 mmol) and 20 mg of Kryptofix 2.2.2 (0.053 mmol) in 0.4 mL of acetonitrile plus 0.2 mL of water followed

by repeated (3 times, 1.5 mL each) azeotropic evaporation with acetonitrile to dryness gave the anhydrous [^{18}F]fluoride complex used in the labeling experiments. Individual step times were 3 min for [^{18}F]fluoride transfer from the cyclotron, trapping and elution from the QMA ion exchange column and 12 min for azeotropic drying, thus resulting in an overall [^{18}F]fluoride processing time of 15 min.

Solvents were purchased from MERCK and used as received. Reagents were purchased from Sigma-Aldrich and used without further purification. 2-Chloroethyl trifluoromethylsulfonate and 2-fluoroethyl trifluoromethylsulfonate were synthesised according to literature procedures [24]. [^{18}F]FMISO was synthesised from a commercially available precursor using the IBA Synthera module.

A Shimadzu HPLC system equipped with a 5 µL injection loop, a SPD-20A UV-Vis detector and two LC-20AD solvent pumps for high pressure mixing of mobile phase was used for quality control of [^{18}F]**1**. The stationary phase was a Phenomenex Gemini C-18, 5µ RP column, 150×4.6 mm. An isocratic 50% acetonitrile/water with 0.1% formic acid mixture was used as the mobile phase at a flow rate of 0.5 mL/min. For the detection of radioactive compounds, the Bioscan FC-4000 dual BGO PET metabolite coincidence detector was used. Identity of the compound was confirmed by comparing the retention time of the radioactive peak with the UV retention time of an authentic sample of [^{19}F]**1**. Specific radioactivity was measured using a mass standard curve of known concentrations of [^{19}F]**1**.

A Shimadzu HPLC system identical to the system described above, equipped with a 20 µL injection loop and a Phenomenex Gemini NX C-18, 5µ RP column, 150×4.6 mm was used for the metabolite studies. Mobile phase composition and flow rate were also identical to the methodology described above.

^{1}H and ^{13}C NMR spectra were recorded in $CDCl_3$ on a Varian Unity 500 NMR spectrometer operating at 500 and 125 MHz respectively. High Resolution Mass Spectrometry (HRMS) was carried out in the positive ion mode on a Finnigan LTQ-FT hybrid linear ion trap (Bremen, Germany) fitted with an electrospray ionization (ESI) source and Fourier Transform Ion Cyclotron Resonance (FT-ICR). Infrared spectra (IR) were recorded on a Perkin Elmer Spectrum One, FT ATR-IR spectrometer.

Synthetic chemistry

F-19 standard synthesis

***N*-(2-fluoroethyl)-4-(4-nitrophenylthio)aniline (4)**

To a stirred solution of 4-(4-nitrophenylthio)aniline (3) (0.87 g, 3.56 mmol, 1 eq.) in dichloromethane (30 mL), was added 2-fluoroethyl trifluoromethylsulfonate (0.70 g, 3.57 mmol, 1 eq.) and 1.1 g of anhydrous potassium carbonate (8 mmol). The mixture

was refluxed under N_2 for 19 h. The reaction mixture was then cooled to room temperature, diluted with H_2O (20 mL) and extracted with diethyl ether (3 x 30 mL). The organic phase was washed with $NaHCO_3$ (3 x 30 mL), H_2O (3 x 30 mL), dried ($MgSO_4$) and concentrated by reduced pressure to give a yellow residue. Purification of the residue by dry flash column chromatography (gradient 2%-80% ether in petroleum spirit) followed by recrystallisation by dicholomethane/n-pentane gave pure **4** as yellow solid (0.35 g, 33.7%) m.p 76.9-77.4°C; TLC R_f 0.29 in ether/hexane (1:1).

^{1}H NMR: 3.52 (2 H, dt, *J* = 26.5 Hz, 4.5 Hz, -N-C*H*$_2$-), 4.30 (1H, m, -N-*H*), 4.67 (2 H, dt, *J* = 47.5 Hz, 4.8 Hz, -C*H*$_2$-F), 6.73 (2 H, d, *J* = 8.5 Hz, C*H*-Ar), 7.09 (2 H, d, *J* = 8.5 Hz, C*H*-Ar), 7.38 (2 H, d, *J* = 8.5 Hz, C*H*-Ar), 8.03 (2 H, d, *J* = 8.5 Hz, C*H*-Ar)

^{13}C NMR: 43.88 (d, *J* = 20.4, -N-*C*H$_2$-), 82.08 (d, *J* = 168.1, -*C*H$_2$-F), 114.17 (*C*H-Ar), 115.99 (*C*-S, Ar), 123.84 (*C*H-Ar), 125.22 (*C*H-Ar), 137.18 (*C*H-Ar), 144.80 (*C*-S, Ar), 148.87 (*C*-N, Ar), 150.98 (*C*-N, Ar)

IR υ_{max}: 1081.9 (C-N), 1332.11, 1501.5 (NO_2)

HRMS *m/z* (ESI+) 292.06755 ($C_{14}H_{13}FN_2O_2SH$ $[M + H]^+$ Calcd 292.06763)

Ethyl 2-((2-fluoroethyl)(4-(4-nitrophenylthio)phenyl)amino)acetate (5)

In a sealed tube, a solution of **4** (250 mg, 0.86 mmol, 1 eq.), ethyl bromoacetate (570 mg, 0.38 mL, 3.42 mmol, 5 eq.) and anhydrous potassium carbonate (350 mg, 2.5 mmol)

in acetonitrile (5 mL) was stirred and heated to 150°C for 20 h. The reaction mixture was then cooled and extracted with diethyl ether (3 x 30 mL). The combined organic phases were washed with $NaHCO_3$ (3 x 50 mL), H_2O (3 x 50 mL), dried ($MgSO_4$) and concentrated under reduced pressure to give a yellow oil. The crude product was purified by automated chromatography using the Biotage Isolera One™ system. A 10 g SNAP™ cartridge and a petroleum spirit(A)/ethyl acetate (B) gradient system (15 min: 0-5%B, 15-41 min: 5-15%B, 41-47 min: 15-100%B) at a flow rate of 12 mL/min was used to elute the target compound. The retention time of **5** under those conditions was 35 min. Evaporation of the solvent gave **5** as a yellow oil (83 mg, 25.7%); TLC R_f 0.426 in ether/hexane (1:1).

^{1}H NMR: 1.29 (3 H, t, *J* = 7.1 Hz, -CH_2-C*H*$_3$), 3.80 (2 H, dt, *J* = 24.5 Hz, 5.0 Hz, -N-C*H*$_2$-), 3.95 (2 H, s, -NC*H*$_2$-CO), 4.23 (2 H, q, *J* =, 7.1 Hz, -O-C*H*$_2$-CH_3), 4.69 (2 H, dt, *J* = 47.1 Hz, *J* = 5.0 Hz, -C*H*$_2$-F), 6.70 (2 H, d, *J* = 8.8 Hz, C*H*-Ar), 7.09 (2 H, d, *J* = 8.9 Hz, C*H*-Ar), 7.39 (2 H, d, *J* = 8.9 Hz, C*H*-Ar), 8.02 (2 H, d, *J* = 8.9 Hz, C*H*-Ar)

^{13}C NMR: 14.08 (-CH_2-*C*H_3), 51.86 (*J* = 21.6 Hz, -N-*C*H_2-), 52.90 (-N-*C*H_2-), 61.44 (-*C*H_2-CH_3), 81.81 (*J* = 169.42 Hz, -*C*H_2-F), 113.27 (*C*H-Ar), 115.82 (*C*-S, Ar), 123.86 (*C*H-Ar), 125.30 (*C*H-Ar), 137.09 (*C*H-Ar), 144.85 (*C*-S, Ar), 149.02 (*C*-N, Ar), 150.78 (*C*-N, Ar), 170.19 (CH_2-*C*OO)

IR υ_{max}: 1084.0, 1384.1 (N-C), 1182.5 (C(=O)-O), 1332.5, 1504.7 (NO_2), 1742.1 (C=O), 2970.5 (C-H) cm^{-1}

HRMS *m/z* (ESI+) 379.11218 ($C_{18}H_{19}FN_2O_4SH$ $[M + H]^+$ Calcd 379.11223)

Ethyl 2-((2-fluoroethyl)(4-(4-nitrophenylsulfinyl)phenyl)amino)acetate ([^{19}F]1)

A solution of $NaIO_4$ (19 mg, 0.087 mmol, 1 eq.) in H_2O (1 mL) was added to a solution of **5** (33 mg, 0.087 g, 1 eq.) in methanol (15 mL) and refluxed under N_2 for 18 h. The reaction was cooled to room temperature, diluted with water (30 mL), extracted with dichloromethane (3 x 30 mL). The organic phases were combined and washed with water (50 mL), dried ($MgSO_4$) and concentrated under reduced pressure to give bright orange oil. The crude product was purified by automated chromatography using the Biotage Isolera One™ system. A 10 g SNAP™ cartridge and a ethyl acetate(A)/petroleum spirit(B) gradient system (7 min: 0-10%B, 7-30 min:10-12%B, 30-31 min: 12-30%B, 31-61 min: 30-40%B, 61-71 min: 40-100%B) at a flow rate of 20 mL/min was used to elute the target compound. The retention time of [^{19}F]**1** under those conditions was 29.2 min. Evaporation of the solvent gave [^{19}F]**1** as a yellow oil (19 mg, 55%); TLC R_f 0.16 in ether/hexane (7:3).

^{1}H NMR: 1.25 (3 H, t, *J* = 7.1 Hz, -CH_2-C*H*$_3$), 3.76 (2 H, dt, *J* = 24.5 Hz, *J* = 4.9 Hz -N-C*H*$_2$-), 4.11 (2 H, s, -NC*H*$_2$-CO), 4.19 (2 H, q, *J* =, 7.1 Hz, -O-C*H*$_2$-CH3), 4.63 (2 H, dt, C*H*$_2$, *J* = 47.0 Hz, 5.0 Hz, -C*H*$_2$-F), 6.59 (2 H, d, *J* = 9.0 Hz, C*H*-Ar), 7.47 (2 H, d, *J* = 9.0 Hz, C*H*-Ar), 7.76 (2 H, d, *J* = 8.8 Hz, C*H*-Ar), 8.28 (2 H, d, *J* = 8.8 Hz, C*H*-Ar)

^{13}C NMR: 14.16 (-CH_2-*C*H$_3$), 51.86 (*J* = 21.1 Hz, -N-*C*H$_2$-), 52.88 (-N-*C*H$_2$-), 61.44 (-*C*H$_2$-CH$_3$), 81.59 (*J* = 170.0 Hz, -*C*H$_2$-F), 112.47 (*C*H-Ar), 124.15 (*C*H-Ar), 125.35

(*C*H-Ar), 128.01 (*C*H-Ar), 131.31 (*C*-S, Ar), 148.98 (*C*-S, Ar), 150.76 (*C*-N, Ar), 153.47 (*C*-N, Ar), 169.75 (CH_2-*C*OO)

IR υ_{max}: 1038.3 (S=O), 1088.3, 1360.8 (N-C), 1198.4 (C(=O)-O), 1343.8, 1590.7 (NO_2), 1738.7 (C=O), 2915.2 (C-H) cm^{-1}

HRMS *m/z* (ESI+) 395.10704 ($C_{18}H_{19}FN_2O_5SH$ $[M + H]^+$ Calcd 395.10715)

Radiolabelling precursor

Ethyl 2-(4-(4-nitrophenylamino)acetate (6)

To a solution of 4-(4-nitrophenylthio)aniline (3) (1.0 g, 4.06 mmol) in acetonitrile (5 mL) in a tube were added ethyl bromoacetate (1.30 g, 0.91 mL, 8.12 mmol, 2 eq.) and anhydrous potassium carbonate (1.6 g, 12 mmol). The tube was sealed and the reaction was heated to 150°C for 18 h. The reaction mixture was then cooled and extracted with diethyl ether (3 x 30 mL). The combined organic phases were washed with $NaHCO_3$ (3 x 50 mL), H_2O (3 x 50 mL), dried ($MgSO_4$) and concentrated under reduced pressure. The crude product was purified by automated chromatography using the Biotage Isolera One™ system. A 25 g SNAP™ cartridge and a petroleum spirit(A)/ethyl acetate(B) gradient system (4 min: 0-8%B, 4-42 min: 8-25%B, 42-52 min: 25-100%B) at a flow rate of 25 mL/min was used to elute the target compound. The retention time of **6** under those conditions was 31.2 min. After evaporation of the solvent and recrystallization

with dichloromethane/n-pentane, **6** was obtained as yellow needles (0.41 g, 31%) m.p 132.4-132.8°C; TLC R_f 0.41 in ether/hexane (1:1).

^{1}H NMR: 1.32 (3 H, t, *J* = 7.1 Hz, -CH_2-C*H*$_3$), 3.97 (2 H, s, NH-C*H*$_2$-CO), 4.28 (2 H, q, *J* = , *J* = 7.1 Hz, -O-C*H*$_2$$CH_3$), 4.61 (1H, s, N*H)*, 6.78 (2 H, d, *J* = 8.6 Hz, C*H*-Ar), 7.10 (2 H, d, *J* = 8.9 Hz, C*H*-Ar), 7.39 (2 H, d, *J* = 8.4 Hz, C*H*-Ar), 8.03 (2 H, d, *J* = 8.9 Hz, C*H*-Ar)

^{13}C NMR: 14.14 (-CH_2-*C*H_3), 45.26 (-NH-*C*H_2-), 61.57 (-*C*H_2-CH_3), 113.99 (*C*H-Ar), 115.93 (*C*-S, Ar), 123.82 (*C*H-Ar), 125.18 (*C*H-Ar), 137.16 (*C*H-Ar), 144.78 (*C*-S, Ar), 148.44 (*C*-N, Ar), 150.98 (*C*-N, Ar), 170.44 (CH_2-*C*OO)

IR υ_{max}: 1217.0 (C(=O)-O), 1341.0, 1505.0 (NO_2), 1737.7 (C=O), 2971.0 (C-H), 3378.8 (N-H) cm^{-1}

HRMS *m/z* (ESI+) 333.09030 ($C_{16}H_{16}N_2O_4SH$ $[M + H]^+$ Calcd 333.09035)

Ethyl 2-((2-chloroethyl)(4-(4-nitrophenylthio)phenyl)amino)acetate (7)

A stirred solution of **6** (0.17 g, 0.51 mmol, 1 eq.), 2-chloroethyl trifluoromethylsulfonate (0.78 g, 3.6 mmol, 7 eq.) and 0.22 g of anhydrous potassium carbonate (1.6 mmol) with acetonitrile (5 mL) was heated to 150^{o}C for 18 h in a sealed tube. The reaction mixture was then cooled and extracted with diethyl ether (3 x 30 mL). The organic phases were combined and washed with $NaHCO_3$ (3 x 50 mL), H_2O (3 x 50 mL), dried ($MgSO_4$) and concentrated under reduced pressure to give a yellow oil. The crude product was purified

by automated chromatography using the Biotage Isolera One™ system. A 10 g SNAP™ cartridge and a petroleum spirit (A)/ethyl acetate(B) gradient system (5 min: 0-5%B, 6-60 min: 5-12%B, 60-77 min: 12-100%B) at a flow rate of 12 mL/min was used to elute the target compound. The retention time of **7** under those conditions was 41.6 min. Evaporation of the solvent gave pure **7** as yellow oil (0.18 g, 86%); TLC R_f 0.50 in ether/hexane (1:1).

^{1}H NMR: 1.26 (3 H, t, *J* = 7.0 Hz, -CH_2-C*H*$_3$), 3.74 (2 H, t, *J* = 7.0 Hz, -N-C*H*$_2$-), 3.82 (2 H, t, *J* = 7.0 Hz, -C*H*$_2$-Cl), 4.17 (2 H, s, -NC*H*$_2$-CO), 4.23(2 H, q, *J* = 7.2 Hz, O-C*H*$_2$-CH_3), 6.70 (2 H, d, *J* = 8.9 Hz, C*H*-Ar), 7.09 (2 H, d, *J* = 9.0 Hz, C*H*-Ar), 7.41 (2 H, d, *J* = 8.9 Hz, C*H*-Ar), 8.04 (2 H, d, *J* = 9.0 Hz, C*H*-Ar)

^{13}C NMR: 14.10 (-CH_2-*C*H_3), 40.30 (-N-*C*H_2-), 53.15 (-*C*H_2-), 53.75 (-*C*H_2-), 61.35 (-O-*C*H_2-CH_3), 113.00 (*C*H-Ar), 115.98 (*C*-S, Ar), 123.78 (*C*H-Ar), 125.45 (*C*H-Ar), 137.09 (*C*H-Ar), 144.78 (*C*-S, Ar), 148.26(*C*-N, Ar), 150.60 (*C*-N, Ar), 170.05 (CH_2-*C*OO)

IR υ_{max}: 1198.0 (C(=O)-O), 1331.5, 1502.6 (NO_2), 1739.0 (C=O), 2970.8 (C-H) cm^{-1}

HRMS *m/z* (ESI+) 395.08267 ($C_{18}H_{19}ClN_2O_4SH$ $[M + H]^+$ Calcd 395.08268)

Ethyl 2-((2-chloroethyl)(4-(4-nitrophenylsulfinyl)phenyl)amino)acetate (2)

A solution of $NaIO_4$ (98 mg, 0.46 mmol, 1 eq.) in H_2O (1 mL) was added to a solution of **7** (180 mg, 0.46 mmol, 1 eq.) in methanol (30 mL) and was refluxed under N_2 for 18 h.

The reaction was cooled to room temperature, diluted with water (30 mL), extracted with dichloromethane (3 x 30 mL). The organic phase were combined and washed with water (50 mL), dried ($MgSO_4$) and concentrated under reduced pressure to give a yellow residue. The crude product was purified by automated chromatography using the Biotage Isolera One™ system. A 10 g SNAP™ cartridge and a petroleum spirit (A)/ethyl acetate(B) gradient system (80 min: 0-80%B, 80-82 min: 80-100%B) at a flow rate of 12 mL/min was used to elute the target compound. The retention time of **2** under those conditions was 70.8 min. Evaporation of the solvent yielded pure **2** as orange-yellow oil (81 g, 43%); TLC R_f 0.15 in ether/hexane (7:3).

^{1}H NMR: 1.26 (3 H, t, *J* = 7.2 Hz, -CH_2-C*H*$_3$-), 3.68 (2 H, t, *J* = 6.9 Hz, -N-C*H*$_2$-), 3.78 (2 H, t, *J* = 6.9 Hz, -C*H*$_2$-Cl), 4.13 (2 H, s, -NC*H*$_2$-CO), 4.32 (2 H, q, *J* = 7.2 Hz, O-C*H*$_2$-CH_3), 6.66 (2 H, d, *J* = 9.0 Hz, C*H*-Ar), 7.49 (2 H, d, *J* = 9.0 Hz, C*H*-Ar), 7.77 (2 H, d, *J* = 8.7 Hz, C*H*-Ar), 8.30 (2 H, d, *J* = 8.8 Hz, C*H*-Ar)

^{13}C NMR: 14.17 (-CH_2-*C*H_3), 40.16 (-N-*C*H_2-), 53.24 (-*C*H_2-), 53.79 (-*C*H_2-), 61.56 (-O-*C*H_2-CH_3), 112.36 (*C*H-Ar), 124.19 (*C*H-Ar), 125.48 (*C*H-Ar), 128.06 (*C*H-Ar), 131.58 (*C*-S, Ar), 149.00 (*C*-S, Ar), 150.10 (*C*-N, Ar), 153.47 (*C*-N, Ar), 169.72 (CH_2-*C*OO)

IR υ_{max}: 1049.4 (S=O), 1204.1 (C(=O)-O), 1340.4, 1505.7 (NO_2), 1727.8 (C=O), 2970.5 (C-H) cm^{-1}

HRMS *m/z* (ESI+) 411.07751 ($C_{18}H_{19}ClN_2O_5SH$ $[M + H]^+$ Calcd 411.07760)

Radiochemistry

Synthesis of [^{18}F]1

The precursor **2** (2 mg, 4.9 µmol) in DMSO (1 mL) was added to the dried K[^{18}F]F kryptofix complex and heated at 100°C for 20 min. After the labelling reaction, 10 mL of water was added to the reaction vessel and the crude reaction mixture was subsequently passed through a C-18 SPE cartridge for trapping of the crude product. The SPE cartridge was rinsed with 10 mL of water before elution with 1 mL of ethanol. The ethanol fraction was purified via semi-preparative HPLC. Semi-preparative HPLC was performed using a Shimadzu LC-10AD isocratic pump equipped with a 5 mL injection loop and a reversed phase column (Phenomenex Luna C-18, 10 µ, 10×250 mm). The mobile phase used was 50/50 ethanol/0.1M ammonium formate at a flow rate of 2 mL/min. Detection of chemical compounds was achieved with a Shimadzu SPD-10A UV detector (254 nm) and a Geiger-Müller tube (type 716; LND, Inc., NY) as radiodetector. The radioactive peak at 17.05 min was collected and reformulated using the solid phase extraction method [25]. The isolated, non-decay corrected yields of radioactivity were 1.18±0.24% (n=27, 2.5±0.5% decay corrected radiochemical yield) based on K[^{18}F]F. Radiochemical purity was >95% and specific activity ranged from 92.7-155.9 GBq/µmol.

LogD measurement

LogD was measured by mixing 3.7 MBq of the radiotracer with 1 g each of 1-octanol and phosphate buffer (0.1 M, pH 7.4) in a test tube. The test tube was vortexed for 3 min at room temperature, followed by centrifugation for 5 min at 10,000 rpm. Two weighed samples (0.5 g each) from the 1-octanol and buffer layers were then measured for radioactivity. The distribution coefficient was calculated from the ratio of cpm/g of 1-octanol to that of buffer.

Stability in saline, human plasma and S9 liver fractions

The *in vitro* stability assays in saline, human plasma and S9 liver fractions were performed as previously described by us [26, 27].

Animal Experiments

All animal experiments were approved by the Austin Health animal ethics committee.

Transplants

SK-RC-52 tumors were first grown by injecting suspensions of 6×10^6 SK-RC-52 cells subcutaneously into the flank of BALB/c nude mice. Tumors were allowed to grow to a size of 300 mm^3, cut into 40 mm^3 pieces and transplanted into the shoulder of BALB/c nude mice. Imaging started when the tumors were 236 mm^3 in size. The maximum tumor size imaged was 994 mm^3.

Small animal imaging

Imaging studies were performed using a Mosaic small animal PET scanner. Animals were injected with 9.25 MBq of radiotracer in 100 µL of the final formulation and anaesthetized using isoflurane delivered by the Minerva Biovet animal imaging system before scanning. The Minerva Biovet system also provides a temperature stabilised environment for the animals during the induction and imaging stages. Two hour dynamic imaging was performed by acquiring 12×10 min frames from the start of tracer injection. For all mice, a 10 min static frame was acquired 2 h post injection. Images were reconstructed using the RAMLA3D algorithm [28]. The resultant PET images where then imported into the PMOD analysis system for Volume of Interest (VOI) analysis.

Oxygen tension measurement

After imaging, animals selected for pO_2 measurement were humanely euthanized and the oxygen partial pressure in the tumor was measured using a polarographic oxygen electrode. Tumor pO_2 was measured with a 2-channel time-resolved luminescence-based optical oxygen-sensing probe (Oxylite 2000; Oxford Optronix, Oxford, UK) or oxylite probe. The probes (230 µm o.d.) were precalibrated by the manufacturer (±0.7 mmHg or < ±10% of actual pO_2, whichever was greater). To further ensure correct pO_2 readings in the experiments, the probe was checked in normal saline, and again in animals just sacrificed to ensure a 0 mm Hg recording.

Results and discussion

Chemistry

Cold standard synthesis

The cold standard [^{19}F]**1** was synthesised in an overall yield of 4.7% in 3 steps starting from commercially available 4-(4-nitrophenylthio)aniline (3), as shown in Figure 2. Reaction of **3** with 2-fluoroethyl trifluoromethylsulfonate resulted in the fluoroethyl aniline **4**. After purification, **4** was reacted with ethyl bromoacetate to form the bis alkylated thioether **5**. Oxidation of **5** with $NaIO_4$ gave the cold standard [^{19}F]**1**.

Precursor synthesis

The precursor **2** was synthesised in an overall yield of 11.4% in 3 steps starting from commercially available 4-(4-nitrophenylthio)aniline (3), as shown in Figure 3. Reaction of **3** with ethyl bromoacetate resulted in the ethyl acetate **6**. After purification, **6** was reacted with 2-chloroethyl trifluoromethylsulfonate to form the bis alkylated thioether **7**. Oxidation of **7** with $NaIO_4$ gave the radiolabelling precursor **2**. We have found that the reaction of **3** with 2-chloroethyl trifluoromethylsulfonate yielded mostly bis-alkylated product and we have therefore decided to react **3** with ethyl bromoacetate first. Since this reaction gave higher yields of the monoalkylated product, we achieved higher overall yields of the radiolabelling precursor **2**using this reaction sequence.

Radiochemistry

Synthesis of [^{18}F]1

The radiolabelling precursor **2** was reacted with dried K[^{18}F]F kryptofix 2.2.2 complex in DMSO at 100ºC for 20 min (Figure 3). The radiotracer [^{18}F]**1** was purified via semi preparative HPLC and reformulated in 10% ethanol/saline. Non-decay corrected yields of radioactivity of the reformulated product were 1.18±0.24% (n=27, 2.5±0.5% decay corrected radiochemical yield) based on K[^{18}F]F. Figure 4 shows the quality control of [^{18}F]**1** and the UV chromatogram of the cold [^{19}F]**1** standard. Radiochemical purity was >95% and specific activity ranged from 92.7-155.9 GBq/μmol. The synthesis time including HPLC purification was 120 min. Figure 5 shows the standard curve obtained by performing serial dilutions (0.1, 1, 10 and 100 μg/mL) of the F-19 standard molecule. After measuring the area under the curve (AUC) of a sample, the formula used to calculate the concentration of cold material in a sample was: conc (μg/mL)=AUC×1.823×10^{-5}.

Attempts to increase the radiolabelling yield by using protic solvents, ionic liquids and bicarbonate based eluent systems have not been successful.

***In vitro* studies**

Lipophilicity

The octanol/water (0.1M phosphate buffer, pH 7.4) distribution coefficient was measured and the logD was calculated to be 2.45 for [^{18}F]**1**, thus indicating that the lipophilicity of this compounds is suitable for crossing cell membranes.

Stability and metabolite studies

The radiotracer was found to be stable in human plasma and saline for a period of 2 h. A cytochrome P450 assay using rat S9 liver fractions also showed that the tracer was more than 80% intact after the 2 h incubation time and did not undergo defluorination.

***In vivo* evaluation of [^{18}F]1**

In vivo testing of the compounds was carried out using transplanted SK-RC-52 tumors as a model for tumor hypoxia [29,30]. Tumors were grown in the shoulder of BALB/c nude mice and tumor sizes were measured using a calliper. Animals were imaged with the novel tracer and [^{18}F]FMISO at different stages of tumor growth, ranging from 236 mm^3 to 994 mm^3. Tumors that were not hypoxic ranged from 236-390 mm^3 (n=4) in size. As expected, the 10 min static images acquired at 2 h post tracer administration showed no uptake with [^{18}F]FMISO or [^{18}F]**1**.

Hypoxic tumors of 6 animals (tumor sizes 632-994 mm^3) received static 10 min imaging at 2 h post injection with both [^{18}F]FMISO and [^{18}F]**1**. The average tumor to muscle ratio at 2 h post injection was 2.27±0.4 for [^{18}F]**1** and 2.59±0.6 for [^{18}F]FMISO. Three animals per radiotracer ([^{18}F]FMISO and [^{18}F]**1**) bearing large, hypoxic tumors

(731, 942 and 994 mm^3) were also imaged dynamically over a period from 0-2 h post injection (12×10 min frames) to measure time activity curves (TACs). The TACs for tumor and muscle have shown that [^{18}F]**1** clears faster from normoxic tissue than [^{18}F]FMISO. Figure 6 shows a typical TAC of muscle and tumor for [^{18}F]**1** and [^{18}F]FMISO of a mouse bearing a 994 mm^3 hypoxic SK-RC-52 tumor.

Due to fast clearance from normoxic tissue, a tumor to muscle ratio of 1 is reached at 20 min post injection with [^{18}F]**1**, whereas this ratio is only observed at 60 min with [^{18}F]FMISO. Imaging with [^{18}F]**1** therefore visualizes hypoxic tumors at earlier time points than [^{18}F]FMISO. Figure 7 shows a direct comparison between the [^{18}F]**1**/[^{18}F]FMISO-PET images obtained at 50 min post tracer administration of a set of two mice (M1, M2) bearing hypoxic SK-RC-52 tumors. The mice were first imaged with [^{18}F]**1** (left set of mice) and then [^{18}F]FMISO on the following day (right set of mice). Tumor volumes were 942 mm^3 for mouse 1 and 994 mm^3 for mouse 2.

In the 50 min post injection [^{18}F]**1** PET images both tumors are clearly visible, whereas [^{18}F]FMISO imaging showed little contrast between tumor and surrounding tissue. An image of a non-hypoxic tumor showing no radiotracer uptake even at 120 min post injection is also given.

The proposed mechanism of trapping in hypoxic cells could potentially result in the loss of the fluorine-18 label. This would lead to increased bone uptake over time due to the well known accumulation of fluorine-18 in this tissue. We have never observed any bone uptake with our F-18 fluoroethyl sulfoxides and therefore conclude that the

formation of an aziridinium ion via displacement of the fluorine-18 label is less favored than the displacement of a chloride or the hydrolysis of an ester moiety.

Conclusion

We have synthesised a novel F-18 labelled 4-nitrophenyl sulfoxide, [^{18}F]**1** and compared its in vivo properties to [^{18}F]FMISO. We have found that [^{18}F]**1** has similar hypoxia selectivity to [^{18}F]FMISO but clears faster from normoxic tissue and it was possible to generate PET images of hypoxic tumors at 50 min post injection. The lipophilicity of this novel radiotracer is in the desired range for PET imaging and the stability towards metabolism by S9 liver fractions make this compound an extremely interesting radiotracer for hypoxia imaging. However, the low labelling yields may limit the widespread use in a clinical setting. Furthermore, the mechanism of uptake of [^{18}F]**1** needs to be elucidated to better understand and potentially further optimise the *in vivo* properties of novel sulfoxide based radiotracers containing an ethyl ester moiety.

Acknowledgments

This work was supported by grants from the National Health and Medical Research Council (NHMRC) grants no. 469002 and 1011418.

References

[1] A.Y. Isa, H. Ward, M.L. West, J. Slevin, J.J. Homer, *Br. J. Radiol.*, **2006**, 79, 791–798

[2] J. Bussink, J.H.A.M. Kaanders, A.J. van der Kogel, *Radiother. Oncol.*, **2003**, 67, 3–15.

[3] H.L. Janssen, K.M. Haustermans, A.J. Balm, A.C. Begg, *Head & Neck*, **2005**, July, 622-638.

[4] S.M. Evans, K.D. Judy, I. Dunphy, W.T. Jenkins, W.T. Hwang, P.T. Nelson, R.A. Lustig, K. Jenkins, D.P. Magarelli, S.M. Hahn, R.A. Collins, S.M. Grady, C.J. Koch, *Clin. Cancer Res.*, **2004**, 10, 8177–8184.

[5] Y. Nagao, S. Sano, M. Ochiai, K. Fuji, S. Nishimoto, T. Kagiya, C. Murayama, T. Mori, Y. Shibamoto, K. Sasai, A. Mitsuyuki, *Chem. Pharm. Bull.*, **1989**, 37, 1951–3.

[6] Z.Y. Sun, E. Botros, A.D. Su, Y. Kim, E. Wang, N.Z. Baturay, CH Kwon, *J. Med. Chem.*, **2000**, 43, 4160-4168.

[7] W.A. Denny, *Lancet Oncol.*, **2000**, 1, 25–29.

[8] Y. Chen, L. Hu, *Med. Res. Rev.*, **2009**, 29, 29-64.

[9] P.J. Hoskin, M.I. Saunders, *Clin. Oncol. (Roy. Coll. Radiol.)*, **1994**, 6, 281–282.

[10] J.H. Chang, M. Wada, N.J. Anderson, D. Lim-Joon, S.T. Lee, S.J. Gong, D.H. Gunawardana, J. Sachinidis, G. O'Keefe, H.K. Gan, V. Khoo, A.M. Scott, *Acta Oncol.*, **2013**, 52, 1723-9.

[11] K. Hendrickson, M. Phillips, W. Smith, L. Peterson, K. Krohn, J. Rajendran, *Radiother. Oncol.*, **2011**, 101, 369–375.

[12] J.G. Rajendran, K.R.G. Hendrickson, A.M. Spence, M. Muzi, K.A. Krohn, D.A. Mankoff, *Eur. J. Nucl. Med. Mol. Imaging*, **2006**, 33, S44-S53.

[13] R. Markus, G.A. Donnan, S. Kazui, S. Read, T. Hirano, A.M. Scott, G.J. O'Keefe, H.J. Tochon-Danguy, J. Sachinidis, D,C. Reutens, *Neuroimage,* **2002**, 16, 425-433.

[14] F. Brady, K.S. Luthra, G.D. Brown, S. Osman, E. Aboagye, A. Saleem, P.M. Price, *Curr. Pharm. Des.*, 2001, 7, 1863-1892.

[15] A. Nunn, K. Linder, H.W. Strauss, *Eur. J. Nucl. Med.*, 1995, 22, 265-280.

[16] S.S. Foo, D.F. Abbott, N. Lawrentschuk, A.M. Scott, *J. Mol. Imag. Biol.*, **2004**, 6, 291-305.

[17] S.T. Lee, A.M. Scott, *Semin. Nucl. Med.*, **2007**, 37, 451-461.

[18] B. Gagel, P. Reinartz, E. DiMartino, M. Zimny, M. Pinkawa, P. Maneschi, S. Stanzel, K. Hamacher, H.H. Coehnen, M. Westhofen, U. Büll, M.J. Eble, *Strahlenther. Onkol.*, **2004**, 10, 616-622.

[19] S.J. Read, T. Hirano, D.F. Abbott, R. Markus, J.I. Sachinidis, H.J. Tochon-Danguy, J.G. Chan, G.F. Egan, A.M. Scott, C.F. Bladin, W.J. McKay, G.A. Donnan, *Ann. Neurol.*, **2000**, 48, 228-235.

[20] L. Dubois, W. Landuyt, L. Cloetens, A. Bol, G. Bormans, K. Haustermans, D. Labar, J. Nuyts, V. Grégoire, L. Mortelmans, *Eur. J. Nucl. Med. Mol. Imaging* **2009**, 36, 209–218.

[21] J. van Loon, M.H.M. Janssen, M. Öllers, H.J.W.L. Aerts, L. Dubois, M. Hochstenbag, A.M Dingemans, R. Lalisang, B. Brans, B. Windhorst, G.A. van

Dongen, H. Kolb, J. Zhang, D. De Ruysscher, P. Lambin, *Eur. J. Nucl. Med. Mol. Imaging*, **2010**, 37, 1663–1668.

[22] C.J. Koch, J.S. Scheuermann, C. Divgi, K.D. Judy, A.V. Kachur, R. Freifelder, J.S. Reddin, J. Karp, J.B. Stubbs, S.M. Hahn, J. Driesbaugh, D. Smith, S. Prendergast, S.M. Evans, *Eur. J. Nucl. Med. Mol. Imaging*, **2010**, 37, 2048–2.

[23] Z. Zha, L. Zhu, Y. Liu, F. Du, H. Gan, J. Qiao, H.F. Kung, *Nucl. Med. Biol.*, **2011**, 38, 501–508.

[24] C.L. Falzon, U. Ackermann, N. Spratt, H.J. Tochon-Danguy, J. White, D. Howells, A.M. Scott, *J. Label. Compd. Radiopharm.*, **2006**, 49, 1089-1103.

[25] C. Lemaire, A. Plenevaux, J. Aerts, A. Del Fiore, C. Brihaye, D. Le Bars, D. Comar, A. Luxen, *J. Label. Compd. Radiopharm.*, **1999**, 42, 63-75.

[26] E. Laurens, S.D. Yeoh, A. Rigopoulos, D. Cao, G.A. Cartwright, G.J. O'Keefe, H.J. Tochon-Danguy, J.M. White, A.M. Scott, U. Ackermann, *Nucl. Med. Biol.*, **2012**, 39, 871-882.

[27] U. Ackermann, D. Sigmund, S. D. Yeoh, A. Rigopoulos, G. O'Keefe, G. Cartwright, J. White, A.M. Scott, H.J. Tochon-Danguy, *J. Label Compd. Radiopharm.* **2011**, 54, 788-794.

[28] J. Browne, A.B. de Pierro, *IEEE Trans. Med. Imaging*, **1996**, 15, 687-699.

[29] N. Lawrentschuk, A.M. Poon, S.S. Foo, L.G. Putra, C. Murone, I.D. Davis, D.M. Bolton, A.M. Scott, *BJU Int.*, **2005**, 96, 540-6.

[30] Lawrentschuk N, Lee FT, Jones G, Rigopoulos A, Mountain A, O'Keefe G, A.T. Papenfuss, D.M. Bolton, I.D. Davis, A.M. Scott, *Urol. Oncol.*, **2011**, 29, 411-420.

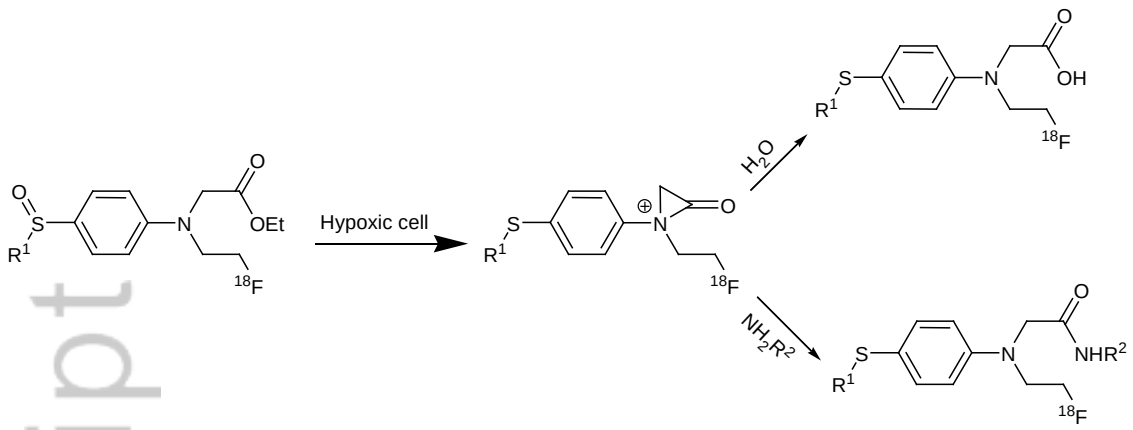

Figure 1: Proposed mechanism of trapping of haloethyl sulfoxides in hypoxic cells

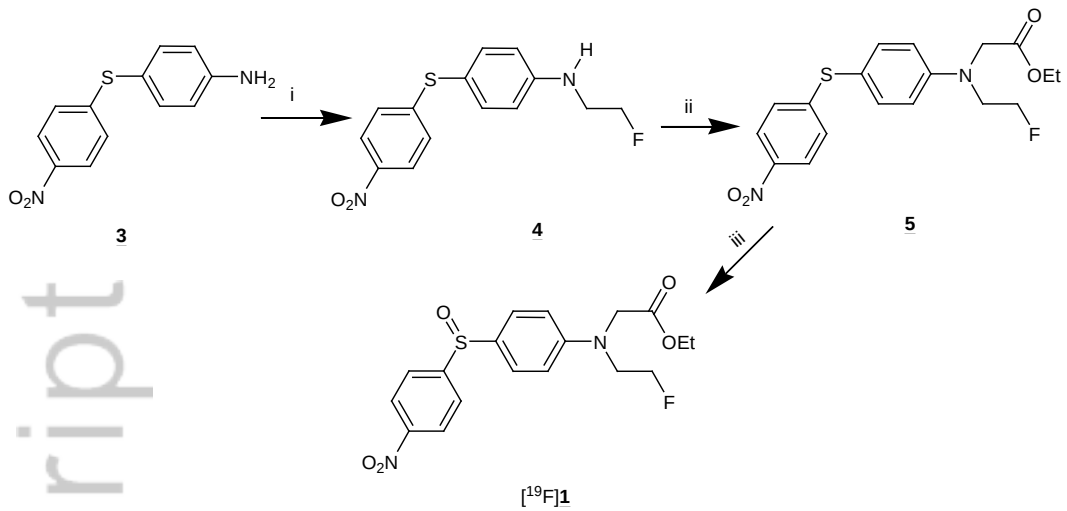

Reagents and conditions: i: 2-fluoroethyl triflate, K_2CO_3, CH_2Cl_2, reflux, 19h; ii: 2-ethyl bromoacetate, K_2CO_3, CH_3CN, 150ºC, 20h; iii: $NaIO_4$, MeOH, reflux, 18h;

Figure 2: F-19 standard synthesis

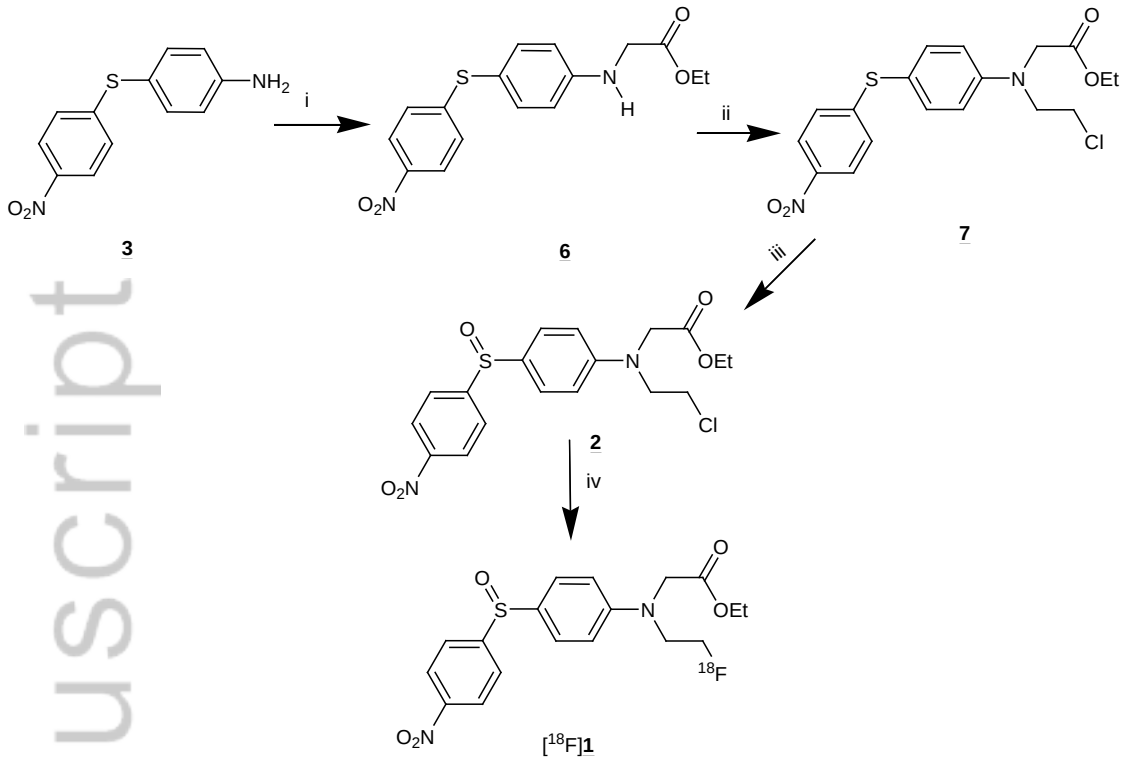

Reagents and conditions: i: 2-ethyl bromoacetate, K_2CO_3, CH_3CN, 150ºC, 18h; ii: 2-chloroethyl triflate, K_2CO_3, 150ºC, 18h; iii: $NaIO_4$, MeOH, reflux, 18h; iv:[^{18}F]KF kryptofix 2.2.2., DMSO, 100ºC, 20 min

Figure 3: Precursor synthesis and radiolabelling reactions

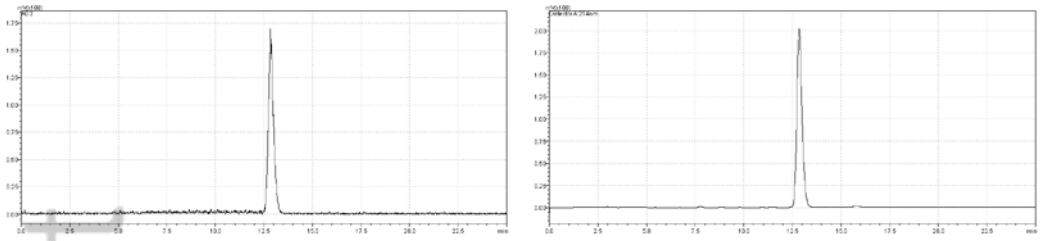

Figure 4: Quality control of [^{18}F]**1**. Radioactive trace (left) and UV trace of F-19 standard (right)

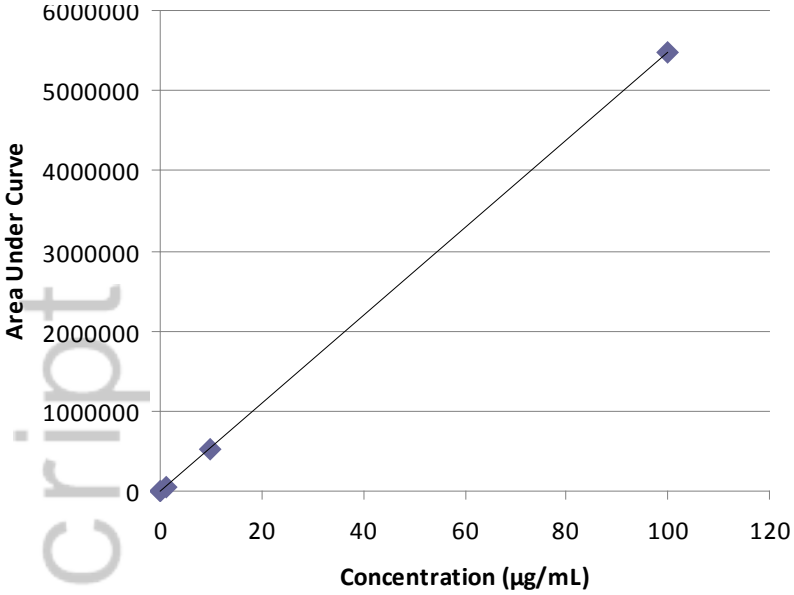

Figure 5: SO501 standard curve

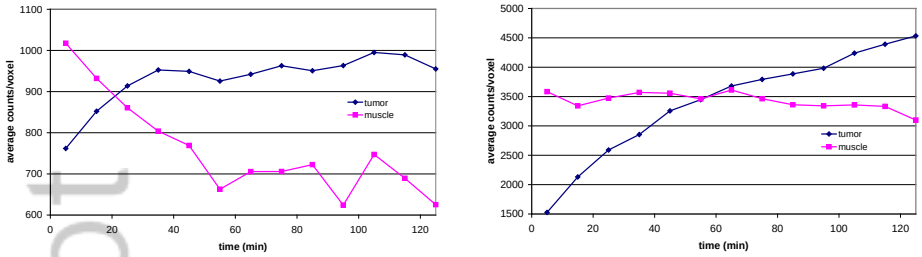

Figure 6: TACs for tumor and muscle for [^{18}F]**1** (left) and [^{18}F]FMISO (right)

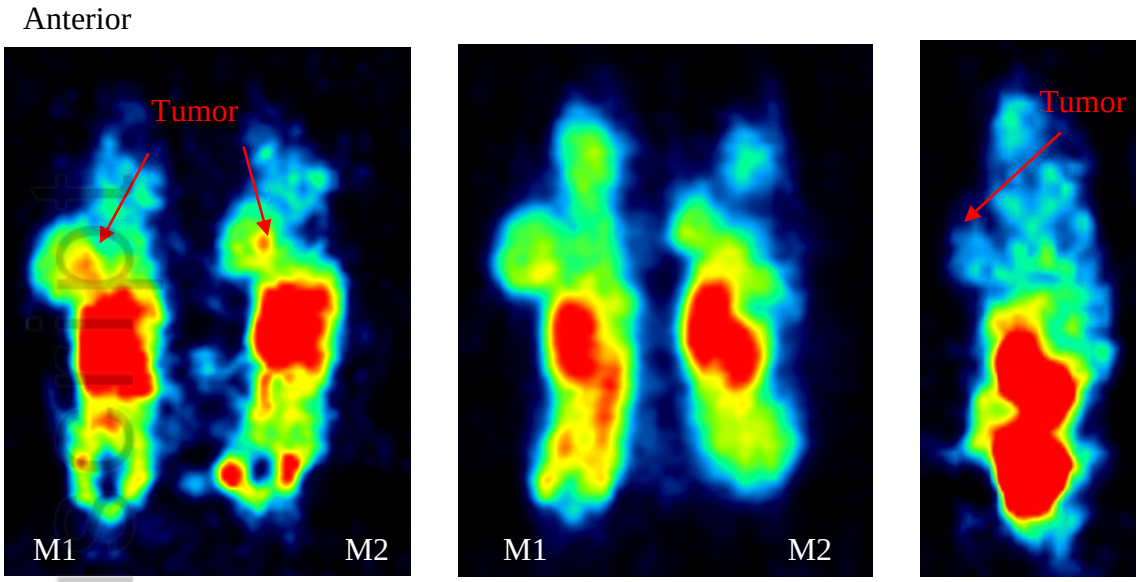

Figure 7: Coronal PET images of [^{18}F]**1** (left) and [^{18}F]FMISO (middle) at 50 min post injection and PET image of a non-hypoxic 360 mm^3 tumor at 120 min post injection

Graphical abstract

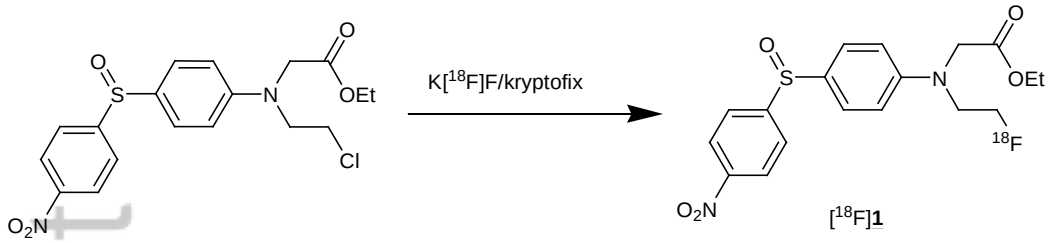

Fluorine-18 radiolabelling of a nitrophenyl sulfoxide and its evaluation in an SK-RC-52 model of tumor hypoxia

Evelyn Laurens[1], Shinn Dee Yeoh[2], Angela Rigopoulos[3], Graeme J. O'Keefe[2], Henri J. Tochon-Danguy[2,4], Lee Wen Chong[1], Jonathan M. White[1], Andrew M. Scott[2,3,4,5], Uwe Ackermann[*2,3,4,5]

[1] School of Chemistry and Bio21 Institute, The University of Melbourne

[2] Department of Molecular Imaging and Therapy, Austin Health, Level 1 HSB, 145 Studley Road, Heidelberg 3084

[3] Olivia Newton-John Cancer Research Institute, Melbourne

[4] School of Medicine, Dentistry and Health Sciences, The University of Melbourne

[5] School of Cancer Medicine, LaTrobe University, Melbourne

[*] Corresponding author

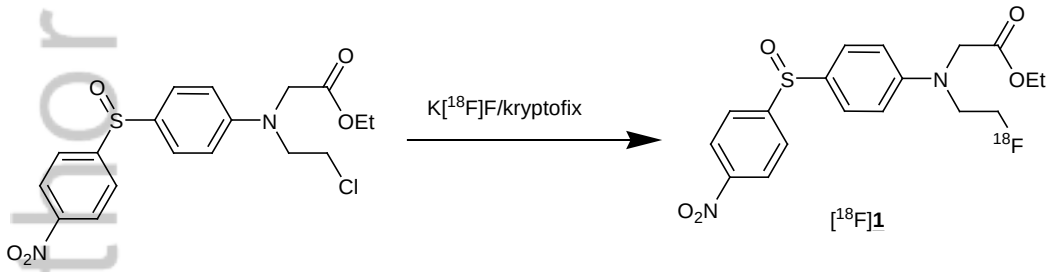

A new nitrophenyl sulfoxide for imaging hypoxia was synthesised via halogen exchange in non-decay corrected yields of radioactivity of 1.18±0.24%. The radiotracer was investigated in our well established SK-RC-52 model of tumor hypoxia and its pharmacokinetics compared to [^{18}F]FMISO. The fast clearance of [^{18}F]**1** from normoxic tissue allows for imaging at earlier timepoints than [^{18}F]FMISO. This compound is an interesting lead structure for further development of hypoxia tracers.